23rd ABCM International Congress of Mechanical Engineering
December 6-11, 2015, Rio de Janeiro, RJ, Brazil

STUDY ON THE PROBLEM OF FILLING A CAVITY IN HYDROELECTRIC TURBINE RUNNERS IN OUT OF POSITION PULSED GMAW WELDING: BEAD GEOMETRY PREDICTION FOR DEPOSITION PLANNING.

José Luis Lázaro Plata
University of Brasília, Departament of Mechanical Engineering, Brasília, D.F., 70.910-900, Brazil
joseph.lazaro@hotmail.es

Edison Andres Arteaga López
University of Brasília, Departament of Mechanical Engineering, Brasília, D.F., 70.910-900, Brazil
edison_arteaga@outlook.com

Guilherme Caribé de Carvalho
University of Brasília, Departament of Mechanical Engineering, Brasília, D.F., 70.910-900, Brazil
gccarval@unb.br

Abstract. *Fatigue crack removal and cavitation erosion phenomena promote the loss of mass in hydroelectric turbine runner blades. Generally, the blade geometry recovery is carried out by means of depositing weld metal to fill the cavities followed by a gridding process to recover the original geometry. Such work is normally carried out manually, thus requiring several hours of highly skilled welders. In the last few years, some attempts have been made to automatizing such repair work, mainly in recovering cavitation erosion cavities. In the case of fatigue crack recovery, manual operation is still the prevalent way of depositing the metal. When thinking about defining the necessary sequence and the distribution of weld beads to fill the cavity with metal, such that the deposition process can be robotized, some problems arise related to the bead section geometry dependence on the welding parameters and on the welding position. Such geometry will strongly influence the number of layers of weld beads needed, considering that the filling process is carried out in layers. In this case, the first problem to be faced is the definition of the distance between parallel beads necessary for the deposition of a maximally flat weld layer. The second problem is the layer thickness that results from the selected distance between parallel beads within a layer. This paper, therefore, addresses the two previously cited problems by developing statistical models that can map the bead section geometry variations due to changes in welding position and in welding parameters for the pulsed GMAW process. A factorial design was used to define the number of weld samples needed for developing the models and welds were carried out in the horizontal position in joints similar to the fillet, although with an angle of 135deg. The joints were rotated about their longitudinal axes in order to achieve different welding positions, ranging from the 1F to the 4F (excluding 3F). The resulting bead geometries were then measured and compared to a parallelogram shape. Models relating the parallelogram height, width and angle of inclination were then produced as functions of the welding parameters and the angle between the gravity vector and the rotation of the bead face.*

Keywords: *Pulsed GMAW; bead geometry modeling; out of position welding*

1. INTRODUCTION

Fatigue crack removal and cavitation erosion phenomena promote the loss of mass in hydroelectric turbine runner blades. Generally, the blade geometry recovery is carried out by means of depositing weld metal to fill the cavities followed by a gridding process to recover the original geometry. Since it is very difficult or even impossible to change a welding position in such large structures, the conventional short circuiting or the pulsed gas metal arc welding process are indicated, taking into account their flexibility and productivity (Xu *et al.*, 2014).

Pulsed GMAW is a promising welding process with the advantage of higher deposition efficiency when compared with conventional GMA welding (Goyal *et al.*, 2009). In out of position welding, the control of the molten pool is a challenge, since the molten metal dynamics is also affected by the gravitational force, which tends to pull the liquid metal towards the gravity vector direction. Many efforts has been made to try to solve this problem, which include applying pulse current power to decrease heat input, thus controlling the pool size (Tham *et al.*, 2012) and controlling the torch position (Alagesan, 2014) to oppose the effect of the gravity force on the molten pool. In order to ensure weld quality on weld bead geometry in all welding positions, the pulsed variation of the GMAW process (P-GMAW) can be considered a good option, further to the might be used GMAW process must be employed in automatic mode in an industry. In such applications, the selection of optimal weld parameters and control of weld bead shape has become essential because it has a significant effect on deposition of welded joints. In position P-GMAW, the weld bead shape is affected not only by weld parameters such as weld current and weld speed, but also by weld position and deposition parameters such as wire feed speed and control of torch position. So, it is very difficult to fix several optimal parameters to get the desired weld bead shape. To achieve this objective, the interrelationship between weld bead geometry and weld parameters requires to be developed. Many efforts have been made to develop statistical models to study this relationship. Xu *et al* (2014) studied the effects of the welding parameters on the weld bead shape in a narrow gap all-position GMA welding process by employing a statistical experimental design method, and linear regression equations were developed. Dong-Yoon (2012) estimated a model for aluminum alloy lap joint welding using hybrid system with laser and scanner head. Badkar *et al* (2012) applied the RSM and central composite design (CCD) to develop a model for laser-herded bead profile and optimized the laser-transformations hardening parameters. Kim *et al* (2011) developed an empirical model for back-bead geometry in root-pass welding of a pipeline. Koleva (2005) studied the relationship between electron beam welding parameters and weld bead shape, and statistical modelling was developed to optimize the parameters. Although several geometry prediction models have been developed by the former authors, only Xu *et al* (2014) and Kim *et al* (2011) mentioned the inclusion of the weld position and one of the independent factors involved in the modelling. Also, none of the cited authors developed models for joints similar to the fillet joint.

When filling a cavity with weld metal by depositing weld layers composed of sequential parallel weld beads, the "joint" geometry expected after the deposition of the first bead of a layer is similar to a fillet joint with and increased included angle. Considering this fact, this paper aims at addressing the problem of defining models that can map the variation in bead geometry as a function of the weld face rotation angle and the welding parameters for the pulsed GMAW process applied to welding fillet joints. A factorial design was used to define the number of weld samples needed for developing the models and welds were carried out in the horizontal position in joints similar to the fillet, although with an included angle of 135 deg. The joints were rotated about their longitudinal axes in order to achieve different welding positions, ranging from the 1F to the 4F. The resulting bead geometries were then measured and compared to a parallelogram shape. Models relating the parallelogram height, width and angle of inclination were then produced as functions of the welding parameters and the angle between the gravity vector and the rotation of the bead face.

2. THE PULSED GMAW PROCESS

Pulsed GMAW is technically a modified spray transfer process. With spray transfer, drops of molten metal are continuously transferred across the arc. However, in the pulsed GMAW process, the power source rapidly switches the welding output from high peak current to low background current. The alternating high pulse current and a lower background current comprise a waveform with an average current below the spray transition current, while maintaining spray droplet transfer qualities, improving transfer stability and out of position welding performance (Joseph *et al.*, 2003). The P-GMAW is versatile, and easily automated. Thus, it is becoming increasingly popular for use in modern robotics and automated industries. Current pulsing has been used to obtain grain refinement in weld fusion zones, which has a positive contribution to mechanical properties. Pulsed GMAW offers better arc characteristics, greatly reduced spatter, less fume generation and lower heat input than spray transfer in steady current GMAW at a given wire feed speed. The lack of any significant spatter will result in less post welding part cleanup, longer-lasting gun parts and a reduction of spatter buildup on jigs, fixtures and torch gas nozzle. The reduction in spatter means that more of the filler metal is transferred to the weld. In many applications, 98 % transfer efficiencies can be obtained, which reduces wasted filler metal (Jeffus, 2011).

2.1 Welding positions

The four basic welding positions are: flat, horizontal, vertical and overhead. Fillet welds can be carried out in all of these positions. Fig. 1 shows the various positions in fillet joints. Each of the positions shown in fig.1 is designated with a number followed by a letter, being the number the indication of the position and the letter, the type of joint.

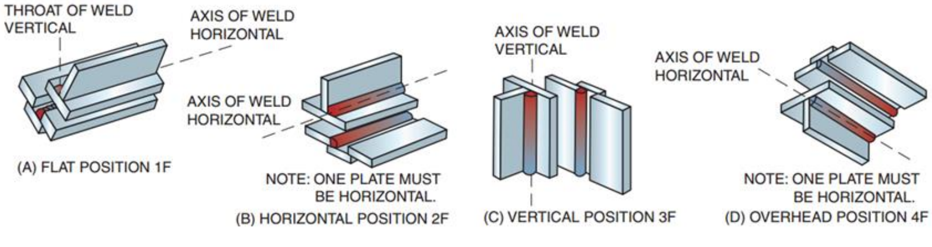

Figure 1. Positions of welding - fillet welds (adapted from Jeffus, 2011)

The 1F position refers to a Fillet weld that is deposited in the flat position. The 1 is used to indicate the flat position and the F indicates a Fillet weld. The number 2 indicates the horizontal position the number 3, vertical position and 4, overhead position. The flat position is the easiest and most desirable position to weld. The other positions are called Out Of Position and are difficult to weld, thus requiring skill to accomplish them well. According to the American Welding Society (2000), the horizontal position occurs when the weld longitudinal axis is approximately horizontal (inclined up to ± 30º from a plane perpendicular to the gravity vector direction) and the rotation of the weld face is limited to the ranges 125º - 150º and 210º - 235º (see Fig. 2). Welding in the horizontal position is a little more difficult to master than flat position. This is due to the tendency of molten metal to flow to the lower side of the joint. The heat from the torch rises to the upper side of the joint. The combination of these opposing factors makes it difficult to apply a uniform deposit to this joint. In vertical position welding, the axis of the weld is approximately vertical. When welding is done on a vertical surface, the molten metal has a tendency to run downward. A weld that is not carefully made will result in a joint with excessive reinforcement at the lower end and some undercutting on the surface of the plates. Overhead welding is carried out from the underside of a joint and the axis of the weld is approximately horizontal. In overhead welding, the metal deposited tends to drop from the plate, causing the bead to have a high crown.

2.2 The join orientation

The join orientation is obtained from the orientation of two vectors, the vector normal to the weld surface, contained into the joint bisection plane, and the vector tangent to the weld axis. This latter also indicates the welding direction (Carvalho, 1997). The axis of rotation of the weld face is determined by a line perpendicular to the weld face at its center which passes through the weld axis. The reference position (0 degrees) or rotation of the weld face invariably points in the direction opposite to that in which the weld axis angle increases. In Fig. 2, when looking at point "P", the angle of rotation of the weld face is measured in a clockwise direction from the reference position (0 degrees) (American Welding Society, 2000). The inclination of the weld axis is measured from the horizontal reference plane toward the vertical reference point. Fig. 2 illustrates the range of positions of welds designated for production fillet welds.

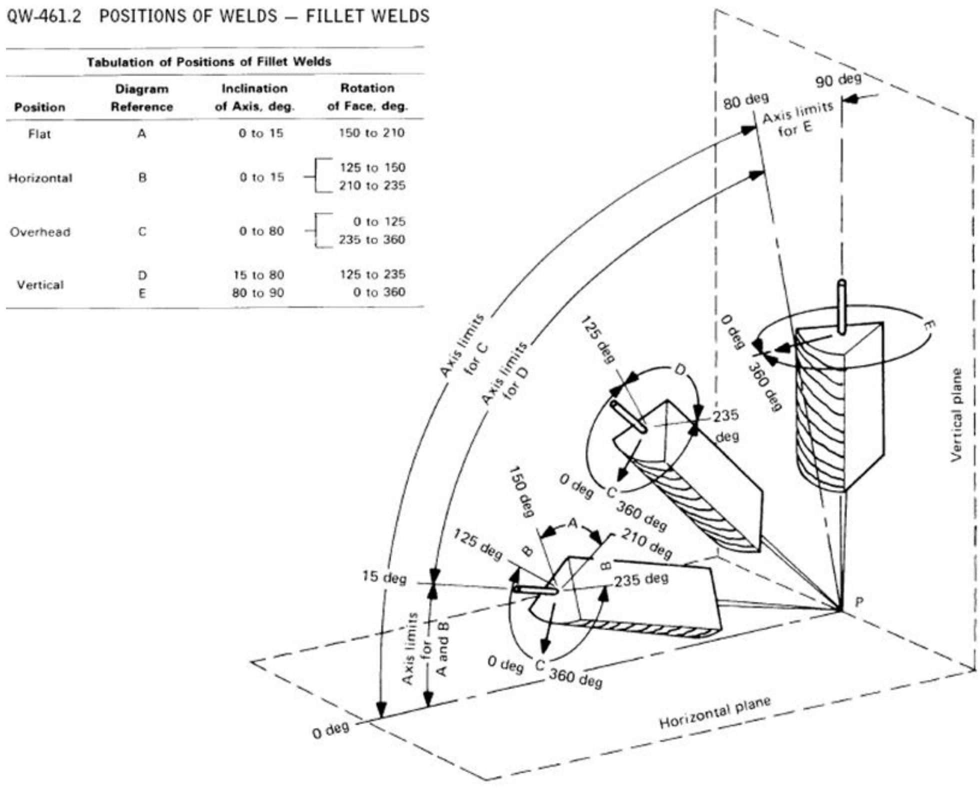

QW-461.2 POSITIONS OF WELDS — FILLET WELDS

Tabulation of Positions of Fillet Welds

Position	Diagram Reference	Inclination of Axis, deg.	Rotation of Face, deg.
Flat	A	0 to 15	150 to 210
Horizontal	B	0 to 15	125 to 150 210 to 235
Overhead	C	0 to 80	0 to 125 235 to 360
Vertical	D	15 to 80	125 to 235
	E	80 to 90	0 to 360

Figure 2. Positions of Fillet Welds (American Welding Society, 2000)

3. METHODOLOGY

The proposed methodology for achieving the objectives was based on several stages in order to meet the requirements involved in experimental research. The phases were structured as follows: Phase 1: Preliminary studies, Phase 2: Development of experiments, Phase 3: Model building.

3.1 Preliminary studies.

A significant number of preliminary bead on plate welding trials, carried out in several positions on 6 mm thick AISI 1020 mild steel plates, helped defining the necessary torch angle (lateral inclination from weld face normal vector) in order to minimize the melt sagging problem, which was in agreement with earlier published results (Alagesan, 2014; Ghosh *et al.*, 2000; Tham *et al.*, 2012). In all experiments, a contact tip to work distance (CTWD) of 16 mm was used. The schematic welding torch positions in the present study is shown in Fig. 3. The experiments were designed based on three welding variables (wire feed speed, welding speed and weld face rotation angle), employing five levels.

Experimental work was separated into two steps. In the first, central composite design was applied to study the influence of the variables on weld bead geometry. The parameter levels and corresponding values are shown in Table 1.

Table 1. Experimental range and levels of the independent variables.

Welding parameters	Coded symbols	Levels				
		-1.682	-1	0	1	1.682
Wire feed speed (m/min)	X1	6.16	6.5	7.0	7.5	7.84
Welding speed (mm/s)	X2	8.32	9.0	10	11	11.68
Weld face rotation angle (deg)	X3	180	216.5	270	323.5	360

In the second step, as shown in Fig. 3, the joint was fixed in seven representative welding positions, corresponding to steps of 30º in the weld face rotation angle, starting at 180º (flat position) up to 360º (overhead). The relationship between welding conditions and weld bead configuration was then investigated for each welding position.

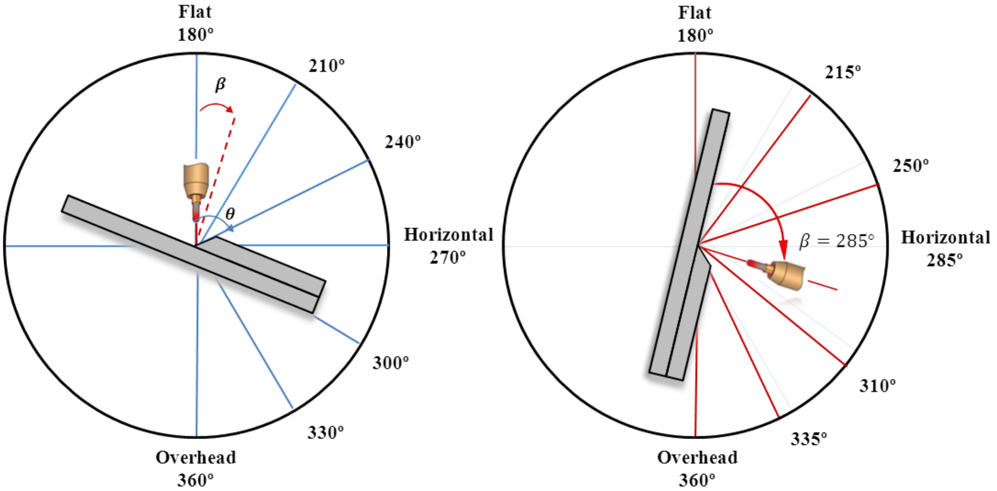

Figure 3. (a) Schematic diagram of welding flat position, (b) Schematic diagram of welding torch angle, horizontal position

Experiments were then carried out and the results enabled the selection of factor levels within their permissible range of variation in other to obtain welds. Table 2 shows the setting conditions of pulsing parameters used for the experimentation.

Table 2. Experimental design plan

Wire feed speed (m/min)	Average current (A)	Period (ms)	Peak time (ms)	Background current (ms)	Peak current (A)	Background current (A)
7	186	6.86	2.4	4.45	380	80
7.5	195	6.4	2.4	3.97	380	80
8	204	6	2.4	3.6	380	80

3.2 Development of experiments

The joint assembly shown in Fig. 5(a) was used to represent the joint geometry expected when depositing beads within a layer after the first weld bead has been deposited. It was formed as a Lap joint assembled from two 6mm thick mild steel plates (50 x 200 mm), where the top plate was chamfered with an angle of 45 deg. After assembling the Lap joint, the resulting joint geometry was similar to a Fillet joint with an included angle of 135 deg, considering that the leg length would always be smaller than the plate thickness. The prepared joints were welded as shown in Fig. 5(b). An inverter welding power source was used for depositing beads using pulsed current GMAW process. Commercial grade Stargold *Clean* 96% Ar + 4% CO_2 was used as the shielding gas. The gas flow rate was set at 15 liters/min. A 1.2 mm diameter metal-cored AWS 410 NiMo tubular wire was used as the consumable electrode. Constant contact tip to work distance (16mm) was maintained throughout the welding operation. The welding position was varied from the 1F to the 4F position by rotating the joint about its longitudinal axis, which was kept in a horizontal orientation.

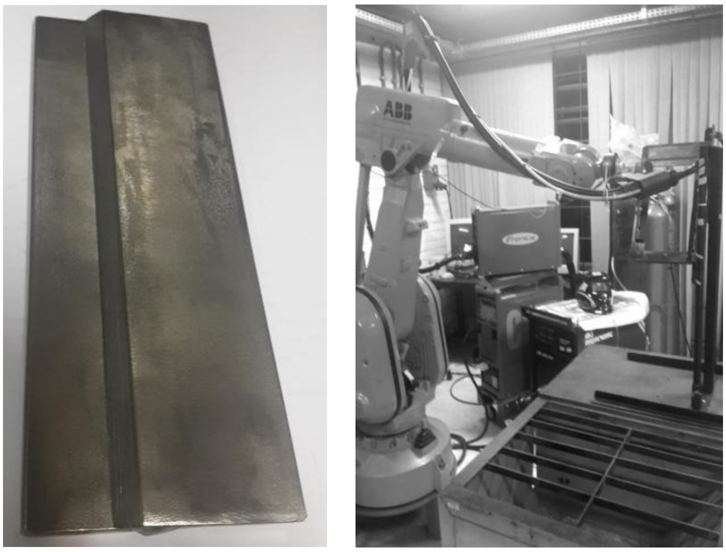

(a) (b)

Figure 4. (a) Welding joint, (b) Photograph of welding experiment

The experiments were conducted as planned by the central composite experimental design (see Table 3 for the designed experimental runs) and the weld bead specimens were prepared as the aforementioned steps to measure the weld bead geometry, as compared to a parallelogram shape (see Fig. 5). Test specimens were cut from the weld beads at half bead length. Weld bead cross section specimens were prepared for macrography analysis, by sanding and polishing using standard procedures. Specimens were then etched with 2% NITAL solution for 20 s. The weld bead geometrical characteristics, relating the parallelogram height (H), width (W) and angle of inclination (α) were then measured with a Tool Profile Projector (Mitutoyo PJ-A3000).

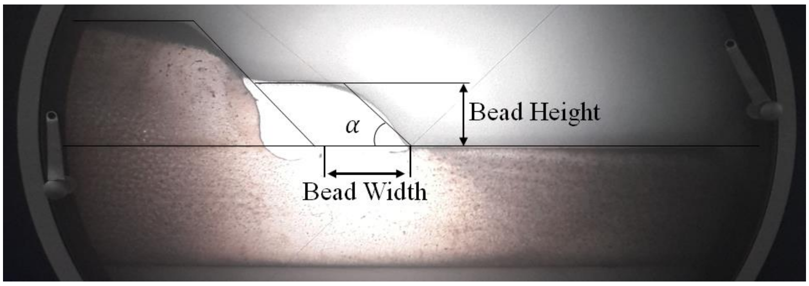

Figure 5. Schematic representation parallelogram height (H), width (W) and angle of inclination (α) parameters measured in GMAW-P

3.3 Model building

After measuring the geometrical features of the weld specimens, three statistical models were produced, considering as dependent variables (responses) the bead height, the bead width and the angle of inclination (α) and, as independent variables (factors), the wire feed speed, the welding speed and the weld face rotation angle. The statistical software

Design-Expert version 9.0.5 (STAT-EASE, Inc., Minneapolis, USA) was used to establish the central composite design matrix (Table 3). Analysis of variance was conducted to determine the significance of the model and the regression coefficients. The quality of polynomial equation was judged by determination coefficient (R^2).

4. RESULTS

Using the central composite design, the experiments with different combination of wire feed speed (m/min), welding speed (mm/s) and weld face rotation angle were carried out. A complete second order model was first tried for each dependent variable and the P-value (level of marginal significance within a statistical hypothesis test) was used as a tool to check the significance of the model and its first order and second order factors. Factors that presented P-value greater than 0.05 were considered insignificant and removed. New second order regression models were then produced considering only the significant factors and the results are shown in Equations (1), (2) and (3).

Table 3. Experimental design matrix and results.

Run	Coded variables			Input variables			Response parameters		
	X1	X2	X3	Wire feed speed (ξ_1) (m/min)	Welding speed (ξ_2) (mm/s)	Weld face rotation angle (ξ_3) (deg)	W (mm)	H (mm)	Angle of inclination (α) (deg)
1	-1	-1	-1	6.5	9	216.5	6.029	3.186	30.20
2	1	-1	-1	7.5	9	216.5	7.385	2.899	28.36
3	-1	1	-1	6.5	11	216.5	4.673	3.083	30.75
4	1	1	-1	7.5	11	216.5	6.404	3.000	29.47
5	-1	-1	1	6.5	9	323.5	4.644	3.801	17.20
6	1	-1	1	7.5	9	323.5	5.513	4.421	17.01
7	-1	1	1	6.5	11	323.5	3.405	2.958	16.94
8	1	1	1	7.5	11	323.5	5.081	3.328	16.52
9	-1.682	0	0	6.16	10	270	4.529	2.708	19.32
10	1.682	0	0	7.84	10	270	6.375	3.297	18.23
11	0	-1.682	0	7	8.32	270	5.971	3.000	19.42
12	0	1.682	0	7	11.68	270	4.933	2.616	17.89
13	0	0	-1.682	7	10	180.0	4.923	3.149	31.65
14	0	0	1.682	7	10	360.0	3.154	4.764	35.20
15	0	0	0	7	10	270	5.250	2.956	18.93
16	0	0	0	7	10	270	5.077	2.750	18.78
17	0	0	0	7	10	270	5.019	2.643	18.10
18	0	0	0	7	10	270	5.423	2.825	17.80
19	0	0	0	7	10	270	5.192	2.702	19.12
20	0	0	0	7	10	270	5.077	2.803	18.45

$$Y_H = 28.88 - 6.364\xi_1 + 1.031\xi_2 - 0.072\xi_3 + 0.348{\xi_1}^2 + 0.000148{\xi_3}^2 + 0.00635\xi_1\xi_3 - 0.00451\xi_2\xi_3 \quad (1)$$

$$Y_W = 51.325 - 9.238\xi_1 - 4.177\xi_2 + 0.046\xi_3 + 0.751{\xi_1}^2 + 0.188{\xi_2}^2 - 0.000109{\xi_3}^2 \quad (2)$$

$$Y_\propto = 171.928 - 0.815\xi_1 + 2.56\xi_2 - 1.033\xi_3 + 0.00179{\xi_3}^2 + 0.018\xi_1\xi_3 \quad (3)$$

, where ξ_1, (m/min) represents the wire feed speed, ξ_2, (m/min), the welding speed and ξ_3, (deg), the weld face rotation angle.

The R^2 obtained for Eq. (1) was 0.9514, for Eq. (2) was 0.9258 and for Eq. (3) was 0.7406. This indicated that 95.14%, 92.58% and 74.06% of the total variation on bead height, the bead width and the angle of inclination, respectively, was attributed to the experimental variables studied. The R^2 value also indicates that only 4.86%, 7.48% and 25.94% of the total variation was not explained by the model. The standard deviations for the three models were 0.16, 0.32 and 3.44, respectively, for Eqs. (1), (2) and (3). The closer the R^2 value to unity and the smaller the standard deviation, the better the model will be as it will give predicted value which is closer to the actual value for the response. This indicated that the predicted value for Y_H would be more accurate and closer to its actual value, compared to Y_W and $Y\propto$. From the statistical results obtained, it was shown that the above models were adequate to predict the weld width and bead height within the range of variables studied. The absolute value of the coefficients of each variable reflecting the importance of the same in terms of their effect on welds bead geometry. In this case, the wire feed speed, the welding speed and the weld face rotation angle presented a very marked effect on weld bead geometry.

A set of 7 pulsed GMA welding experiments in the 1F to the 4F positions was carried out for validation purposes, according to the design matrix shown in Table 4. Using the 1F welding position one can achieve a difference in height and width in the weld bead compared with that for the 2F welding position when using the same welding parameters.

Table 4. Welding position

Run	Input variables			Bead Height, H			Bead Width, W			Angle of inclination, α		
	ξ_1 (m/min)	ξ_2 (mm/s)	ξ_3 (deg)	$H_{predicted}$ (mm)	$H_{measured}$ (mm)	Error (%)	$W_{predicted}$ (mm)	$W_{measured}$ (mm)	Error (%)	$\alpha_{predicted}$ (deg)	$\alpha_{measured}$ (deg)	Error (%)
1	7.5	11	180	3.6	3.5	3.2	5.0	5.4	7.4	23.8	21.9	8.7
2	7.5	11	210	3.0	3.0	1.7	5.2	5.5	5.5	21.5	19.1	12.6
3	7.5	11	240	2.6	2.5	4.0	5.1	5.3	3.6	20.2	19.0	6.2
4	7.5	11	270	2.5	2.5	1.2	4.3	4.6	5.7	19.4	21.3	9.0
5	6.5	11	300	2.5	2.5	2.0	3.9	4.3	9.7	18.0	19.9	9.5
6	6.5	11	330	2.8	2.7	4.1	3.4	3.7	8.7	19.9	18.0	10.6
7	6.5	11	360	3.4	3.4	0.6	2.6	2.7	3.9	22.8	20.4	11.8

From the experiments, it was possible to observe that the bead width, W, increases with the increase in ξ_3 from 0 to 300°. When ξ_3 is more than 270°, the bead width reduces as ξ_3 increases. This is attributed to the fact that the molten metal flows below the arc by the effect of gravity and the arc force makes the molten pool surface depressed. As shown in Table 4, the maximum value of W for all values of ξ_3 was obtained when ξ_3 = 270°. Also, it was observed that the bead height, H, decreases as welding position goes from the 1F to the 2F (from 180 to 270°), and then it increases with the further increase in welding position (from the 2F towards the 4F). This is supposed to happen due to the fact that, in out of position welding, the control of the molten pool is a challenge, since the molten metal dynamics is also affected by the gravitational force, which tends to pull the liquid metal towards the gravity vector direction.

5. CONCLUSION

From the statistical results obtained, it was shown that the above models were adequate to predict the weld width and bead height within the range of variables studied. The absolute value of the coefficients of each variable reflecting the importance of the same in terms of their effect on weld bead geometry, whereby for the models: bead height and bead width the responses had an R^2 above 0.9, different to the model angle of inclination, where the responses had an R^2 above 0.75. In this case, the wire feed speed, the welding speed and the weld face rotation angle presented a very marked effect on weld bead geometry. Increase in the wire feed speed gives rise to the volume of molten metal at per-unit-length increase, so the weld height increases. Also, it was observed that the bead height, H, decreases as welding position goes from the 1F to the 2F, and then it increases with the further increase in welding position (from the 2F towards the 4F).

6. REFERENCES

Alagesan, R., and Kumar, T. S., 2014 Optimization of welding cycle time by establishing full gmaw process (stt and p-gmaw) through a newly designed semi-automatic welding positioner. *International Journal of Research in Engineering and Technology,* Vol 6, no 3, p. 60-66

American Welding Society., 2000. Welding Inspection Handbook. American Welding Society, LeJeune Road, Miami, Florida 33126, 3rd Edition.

Badkar, D. S., Pandey, K. S., and Buvanashekaran, G., 2012. Application of the central composite design in optimization of laser transformation hardening parameters of commercially pure titanium using Nd: YAG laser. *The International Journal of Advanced Manufacturing Technology*, Vol 59, n. 1-4, p. 169-192.

Box, G.E.P., Hunter, J.S. and Hunter, W.G., 2005. *Statistics for Experimenters: Design, Innovation, and Discovery*. Wiley-Interscience, Hoboken, New York, 2nd Edition.

Carvalho, G. C., 1997. *An adaptive control system for off-line programming in robotic gas metal arc welding*. Ph.D. thesis, Cranfield University, Cranfield UK.

Christensen, K. H., Srensen, T., and Kristensen, J. K., 2005. Gas metal arc welding of butt joint with varying gap width based on neural networks. *Science and Technology of Welding & Joining*, Vol. 10, no 1, p. 32-43.

Dong-Yoon, K. I. M., and Young-Whan, P. A. R. K., 2012. Weldability evaluation and tensile strength estimation model for aluminum alloy lap joint welding using hybrid system with laser and scanner head. *Transactions of Nonferrous Metals Society of China*, Vol 22, s596-s604.

Ghosh, P. K., Gupta, S. R., and Randhawa, H. S., 2000. Characteristics of a pulsed-current, vertical-up gas metal arc weld in steel. *Metallurgical and Materials Transactions A*, Vol. 31, no 9, p. 2247-2259.

Goyal, V. K., Ghosh, P. K., and Saini, J. S., 2009. Analytical studies on thermal behaviour and geometry of weld pool in pulsed current gas metal arc welding.*Journal of materials processing technology*, Vol. 209, no 3, p. 1318-1336.

Joseph, A., Harwig, D., Farson, D. F., and Richardson, R., 2003. Measurement and calculation of arc power and heat transfer efficiency in pulsed gas metal arc welding. *Science and Technology of Welding & Joining*, Vol. 8, no 6, p. 400-406.

Jeffus, L., 2011. *Welding: Principles and Applications*. Delmar Cengage Learning, New York, 7th Edition.

Kim, J. S., Kim, I. S., Na, H. H., and Lee, J. H., 2011. An Experimental study on Prediction of Back-bead Geometry in Pipeline Using the GMA Welding Process. *Journal of the Korean Society of Manufacturing Technology Engineers*, Vol 20, no 1, p. 74-80.

Koga, S., Inuzuka, M., Nagatani, H., Iwase, T., Masuda, H., and Ushio, M., 2000. Study of all position electron beam welding process for pipeline joints. *Science and Technology of Welding & Joining*, Vol 5, no 2, p. 105-112.

Koleva, E., 2005. Electron beam weld parameters and thermal efficiency improvement. *Vacuum*, Vol. 77, no 4, p. 413-421.

Montgomery, D. C., 1983. *Design and Analysis of Experiments*. John Wiley & Sons, New York, 2nd Edition.

Tham, G., Yaakub, M. Y., Abas, S. K., Manurung, Y. H., and Jalil, B. A., 2012. Predicting the GMAW 3F T-Fillet geometry and its welding parameter. *Procedia Engineering*, Vol 41, p. 1794-1799.

Xu, W. H., Lin, S. B., Fan, C. L., Zhuo, X. Q., and Yang, C. L., 2014. Statistical modelling of weld bead geometry in oscillating arc narrow gap all-position GMA welding. *The International Journal of Advanced Manufacturing Technology*, Vol. 72, no 9-12, p. 1705-1716.

7. RESPONSIBILITY NOTICE

The authors are the only responsible for the printed material included in this paper.